JOURNAL OF MATERIALS SCIENCE 30 (1995) 5335–5346

In situ SEM studies on the effects of particulate reinforcement on fatigue crack growth mechanism of aluminium-based metal-matrix composite

M. J. HADIANFARD, Y.-W. MAI
Centre for Advanced Materials Technology (CAMT), Department of Mechanical and Mechatronic Engineering, University of Sydney, Sydney, New South Wales 2006, Australia

The effects of particulate reinforcement on the fatigue behaviour and fatigue mechanisms of two 6061 aluminium-based metal-matrix composites (MMCs) in three different heat-treatment conditions were studied *in situ* with a scanning electron microscope and compared to the unreinforced alloy in the as-received condition. It was observed that the fatigue properties of the MMCs were influenced by the ceramic particles in two ways: firstly the particles increased the fatigue stress intensity threshold mainly by crack-deflection and crack-closure mechanisms, and secondly, the particles raised the fatigue crack growth rates in the Paris region by providing an easy crack path. The effect of ageing was small on the fatigue stress intensity threshold of MMCs, but for the peak-aged MMCs the fatigue crack growth rates in the Paris region were faster. The mechanism of fatigue crack growth was largely associated with the matrix/particle interface and the linkage with subcracks initiated ahead of the main crack at high applied stress intensity factors.

1. Introduction

During the last three decades, metal-matrix composites (MMCs) have emerged as an important class of materials. Therefore, a substantial research effort has been directed towards a better understanding of their behaviour under different loading conditions. MMCs have a special combination of room and elevated temperature strength, modulus and dimensional stability.

Many applications of metal-matrix composites involve cyclic loading. Therefore, there is a need to understand the fatigue resistance of these materials to establish a data base for efficient design under cyclic fatigue. Compared with corresponding wrought aluminium alloys, particulate-reinforced MMCs demonstrate a lower crack propagation resistance but a higher or similar threshold stress intensity factor [1, 2]. Improvements in fatigue strength by 50%–70% for 6061 and 7075 Al alloy have been reported by reinforcing these alloys with SiC whiskers [3]. Shang and Ritchie [4] studied fatigue crack growth rates of 15 and 20 vol% fine and coarse SiC-reinforced over-aged Al–Zn–Mg–Cu alloys and compared the results with those of the unreinforced alloy. The data showed three different regimes, each characterized by a dominant crack extension mechanism. At near threshold levels the coarse SiC composites showed crack growth rates more than two orders slower than the unreinforced alloy and a threshold 28% lower. The fine SiC composites gave similar results as the unreinforced alloy. Here the crack avoided the reinforcement particles leading to better crack resistance in the fine SiC composites. At intermediate growth rates, crack growth resistance was somewhat improved in the composites. This was the result of a mutual competition of SiC particles fractured ahead of the crack tip and crack bridging. Finally, at very high crack growth rates ($> 10^{-6}$ m cycle^{-1}) the crack resistance was superior in the unreinforced alloy due to the much lower toughness of the composites. Yau and Mayer [1] found slower fatigue crack growth rates for SiC/6061 Al MMC compared to the unreinforced alloy at the near-threshold and intermediate ranges but faster at high ΔK level. Davidson [5] in his experiments on a 15 vol% SiC/Al MMC, observed that for fatigue cracks growing at ΔK near threshold, deformation of the matrix was not affected by the presence of SiC particles due to the small plastic zone ahead of the crack tip. At higher ΔK values, deformation was significantly altered by the particles because the larger plastic zone encompassed more particles. It was suggested that the change in matrix deformation characteristics had influenced the fatigue crack growth of MMCs at high values of ΔK. It was also found that ΔK_{th} values were relatively insensitive to the matrix ageing condition and were similar for several different SiC volume fractions [6]. Christman and Suresh [7] reported that ageing treatment had very little effect on the threshold value and the near threshold fatigue crack growth in an SiC_w/2124 Al composite.

The main objective of this work was to gain a fundamental understanding of how the fatigue process in MMCs is affected by the reinforcement particles, microstructure and ageing conditions. Particular

0022–2461

emphasis has been placed on the mechanisms of fatigue crack growth using an *in situ* SEM fatigue technique. This experimental method has obvious advantages over the commonly used direct current/potential drop [8], direct optical [9], compliance measurements [2] or replication techniques [10] in determining fatigue crack growth mechanisms and crack tip/particulate interactions. The superior resolution afforded by the SEM provides further advantage over existing optically based systems. *In situ* SEM shows greater detail of crack microstructure interactions and produces quantitative information on the crack tip characteristics.

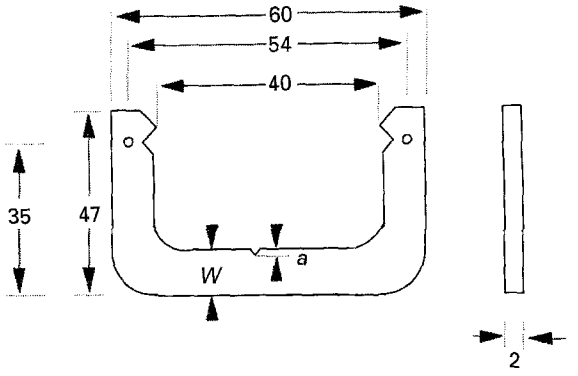

Figure 1 The *in situ* SEM fatigue specimen. Dimensions in mm.

2. Experimental procedure

2.1. Material

Two 6061 Al alloy matrix with 20 vol % particulate-reinforced composites were studied: Duralcan–20% (D20) reinforced with angular alumina (average particle size 18.7 μm) and Comral-85 (C85) reinforced with alumina microspheres (average particle size 17.5 μm). The third material studied was the unreinforced matrix of Comral-85 (6061 Al alloy). All three materials were produced by liquid metallurgy and extruded to a 75 mm wide plate, either 12.5 or 25 mm thick. The D20 and C85 composites were tested in three different conditions: as-received condition (as-extruded), peak-aged condition (T6) and after long-term thermal exposure, while the 6061 Al alloy was tested only in the as-received condition.

2.2. Heat treatment

To produce T6 condition, the MMCs were solution treated at 530 °C for 1.5 h, cold-water quenched and naturally aged for 24 h, followed by artificial ageing at 175 °C for 8 h. For the thermal exposed specimens, peak-aged MMCs were heated at 300 °C for 110 h followed by air cooling.

2.3. Experimental technique

Horseshoe-shaped specimens, 2 mm thick and 10 mm wide, were used. A V-notch was machined perpendicular to one specimen edge to a non-dimensional notch length of a/W between 0.2 and 0.4, where W ($= 10$ mm) is the specimen width. The notch was introduced by a 360 μm wide diamond wafer blade. The specimens were machined in the L–T orientation and polished to 1/4 μm with diamond paste and mounted on the stage. Fig. 1 shows the specimen shape and dimensions.

In situ fatigue observation on the surface of the horseshoe-shaped specimen was performed at room temperature. The *in situ* fatigue testing equipment was designed and made in Denmark by Aalborg University. The principal components of the equipment are the specimen, supporting structure, load cell, load transducers and hydraulic pressure supply [11]. The equipment was especially designed so that the specimen stage, supporting structure, load cell and load transducer could be inserted into the vacuum chamber of a Phillips 505 scanning electron microscope. Fig. 2

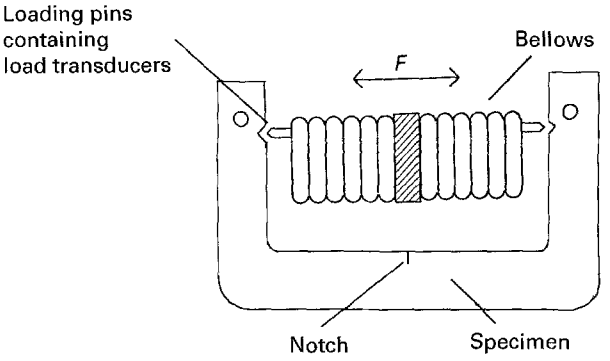

Figure 2 The load cell and loading pins.

shows a schematic diagram of the load transducer and specimen.

A cyclic load, F, was applied by bellows operated by a closed elastic hydraulic system external to the SEM chamber. The main pressure and pressure range could be independently adjusted. A maximum pressure of 13 bar could be used with this system. Tests were run with 15–20 kV accelerating voltage and the sample surface normal to the beam. The crack propagated under constant amplitude tensile cyclic load according to the ASTM E647 standard with a stress ratio, R, equal to zero (i.e. a minimum load of zero). The maximum frequency applied was 15 Hz. Crack growth was monitored by a series of photographs and a video tape recorder. Because the specimen was subjected to a bending moment and an axial force, the stress intensity factor K values were calculated from measurements of the applied load and crack length according to the following equation [12]

$$K_1 = \sigma\sqrt{\pi a}(1.12 - 0.231\alpha + 10.55\alpha^2 - 21.72\alpha^3 + 30.39\alpha^4) + 6M(\sqrt{\pi a}/TW^2)(1.12 - 1.4\alpha + 7.33\alpha^2 - 13.08\alpha^3 + 14.0\alpha^4) \quad (1)$$

where $\alpha = a/W$, T is specimen thickness, M is the bending moment and σ is axial stress. After fatigue testing the surfaces of the specimens were examined by an optical microscope equipped with a computer image analyser.

3. Results

3.1. Unreinforced alloy

In situ fatigue observations were made with the aid of a series of micrographs which showed the crack

growth behaviour. At low ΔK ($da/dN < 10^{-6}$ mm cycle^{-1}) crack growth was accompanied by microcracking ahead of the main crack tip and near intermetallic inclusions (Fig. 3). The crack path at low ΔK levels was therefore characterized by microcracking ahead, behind and around the main crack (Fig. 4). At high ΔK levels, however, when $da/dN > 10^{-6}$ mm cycle^{-1}, the main crack was observed growing with massive deformation ahead of its tip. Within the deformation zone, many microcracks formed, as shown in Fig. 5. After repeated loading and unloading, the main crack finally linked up with these microcracks and formed a continuous crack. A large number of crack branches were observed in the specimen at high levels of ΔK. Fig. 6 shows a crack profile at high ΔK levels. Fatigue crack growth in the unreinforced alloy in the as-received condition was characterized by large crack tip opening displacement and pronounced crack tip branching.

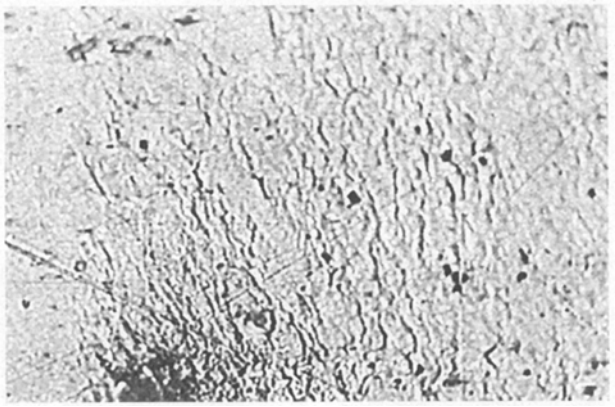

Figure 3 Microcracks ahead of crack tip in the unreinforced alloy x 520.

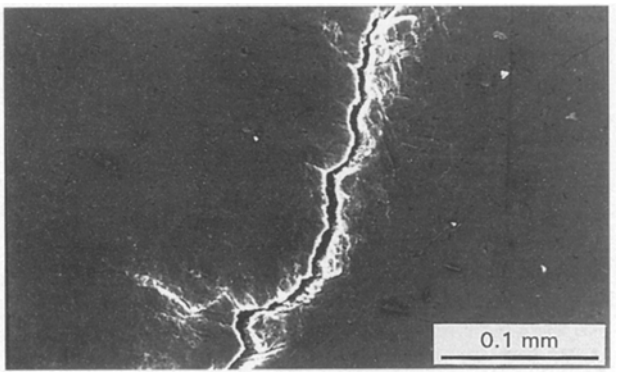

Figure 4 Crack path at low levels of ΔK in the unreinforced alloy.

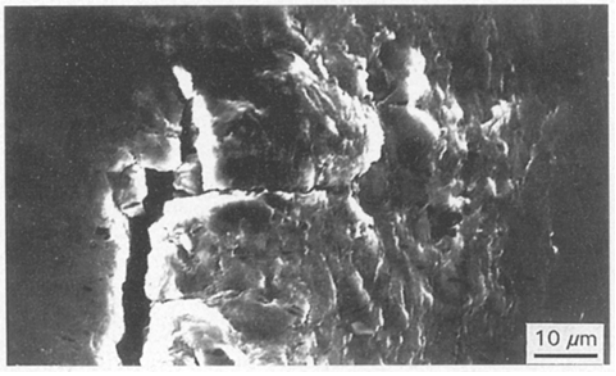

Figure 5 Plastic deformation and microcrack forming at a crack tip in the unreinforced alloy at high ΔK values.

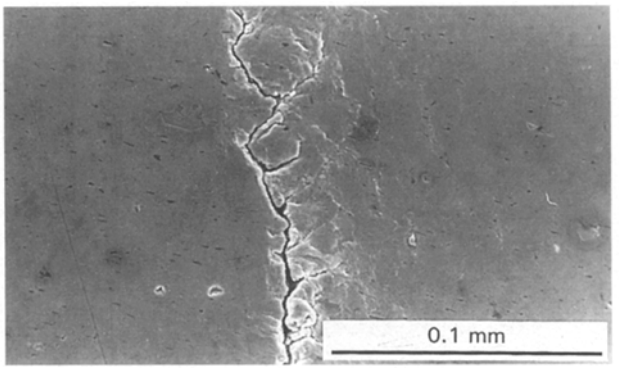

Figure 6 Crack path at high levels of ΔK in the unreinforced alloy, showing microcracks along the crack path.

3.2. Duralcan–20% (D20) composite

At low levels of ΔK, fatigue crack growth in the as-received material was usually associated with the metal/particle (m/p) interface. The crack also passed through areas of low-density particulates areas (Fig. 7). At this level of ΔK, only a single crack tip, i.e. crack growth took place along a single front with multiple micro-branching occurring on both sides of the crack plane, Fig. 8a, was observed and no other microcracks near or ahead of main crack tip were found. In addition, the crack tip displayed minor crack tip branching. Coarse alumina particles (> 20 μm) were also observed to fracture due to crack growth. A sequence of photographs taken at low ΔK (Fig. 9) shows the progression of the crack through the composite and crack tip deflection due to the weak m/p interface. Initially, it seems that the crack will pass through the particle (Fig. 9a and b), but finally it changes direction and links up with microcracks already produced in the m/p interface of the particle (Fig. 9c). Then the crack continues to grow, passing through the m/p interface of the next particle (Fig. 9d). At high ΔK levels, crack growth was characterized by subcracking ahead of the crack tip and linking subcracks to the main crack (Fig. 10). Fig. 11 shows crack-tip deflection at high levels of ΔK due to the main crack linking up with sub-cracks in the fractured particles. When large sub-cracks were formed ahead of the main crack it became difficult to determine the location of the main crack tip. In addition, at this level of ΔK, multiple crack tips (initial micro-branching followed by crack growth along several fronts originated from one or more microcracks and one of which became the main crack path, Fig. 8b) could be formed. Fig. 12 shows two crack tips in the D20 as-received specimen. Multi-crack tip phenomenon has also been reported by Davidson [5] in 2014 Al/15 vol % SiC at high levels of ΔK. At high ΔK the fatigue crack tended to pass through areas with a slightly higher density of particles (Table I).

In D20 peak-aged (T6) condition, the same phenomena as found in the as-received condition were

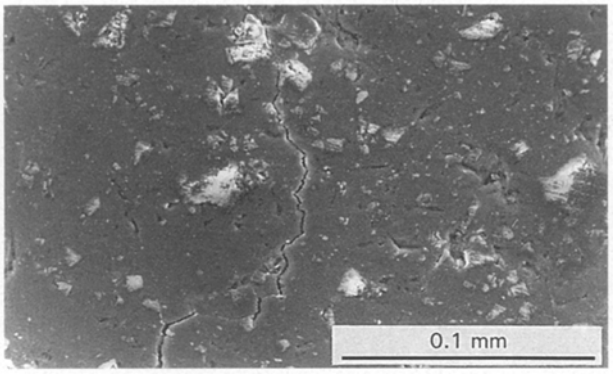

Figure 7 The crack profile at low ΔK level in as-received D20.

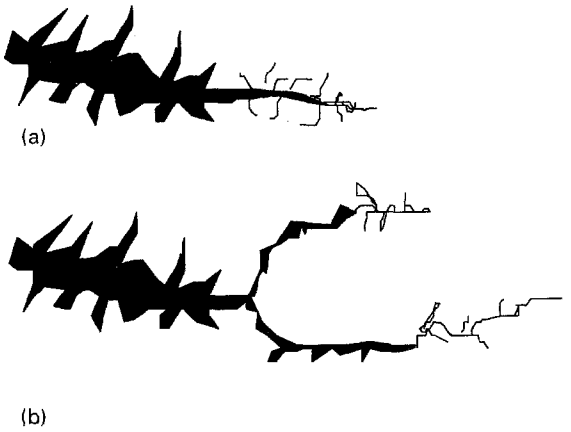

Figure 8 Different crack tip shapes: (a) single crack tip, and (b) multiple crack tips.

observed. At low levels of ΔK a single crack propagated through areas with a slightly lower particle density (Table I); fatigue crack growth was strongly associated with the m/p interface. At high levels of ΔK crack growth was found to be caused by subcracking ahead of the crack tip and linking of the main crack to the subcracks. Multiple crack tips and crack growth through areas of slightly higher particle density were also observed. In contrast with the as-received specimen subcracking was mostly produced at the m/p interface of particles ahead of the crack tip (Fig. 13). Results of image analysis on the crack path in different specimens (Table II) show that the percentage of debonded particles increased in the T6 specimen. This result together with the fatigue mechanisms observed especially at high levels of ΔK, indicate that heat treatment to peak-aged condition made the m/p interface weaker than the as-received condition and produced more debonding particles associated with fatigue crack growth.

Fig. 14 shows part of the fatigue crack path in D20 thermally exposed specimen. In this specimen crack growth was strongly associated with debonding at the m/p interface for both low and high levels of ΔK. Although a few fractured particles were observed during fatigue crack growth most of the reinforcement particles did not appear to crack, but were debonded from the matrix at the m/p interface. At low ΔK values, the crack grew in areas with a low density of reinforcement particles (Table I), and passed through

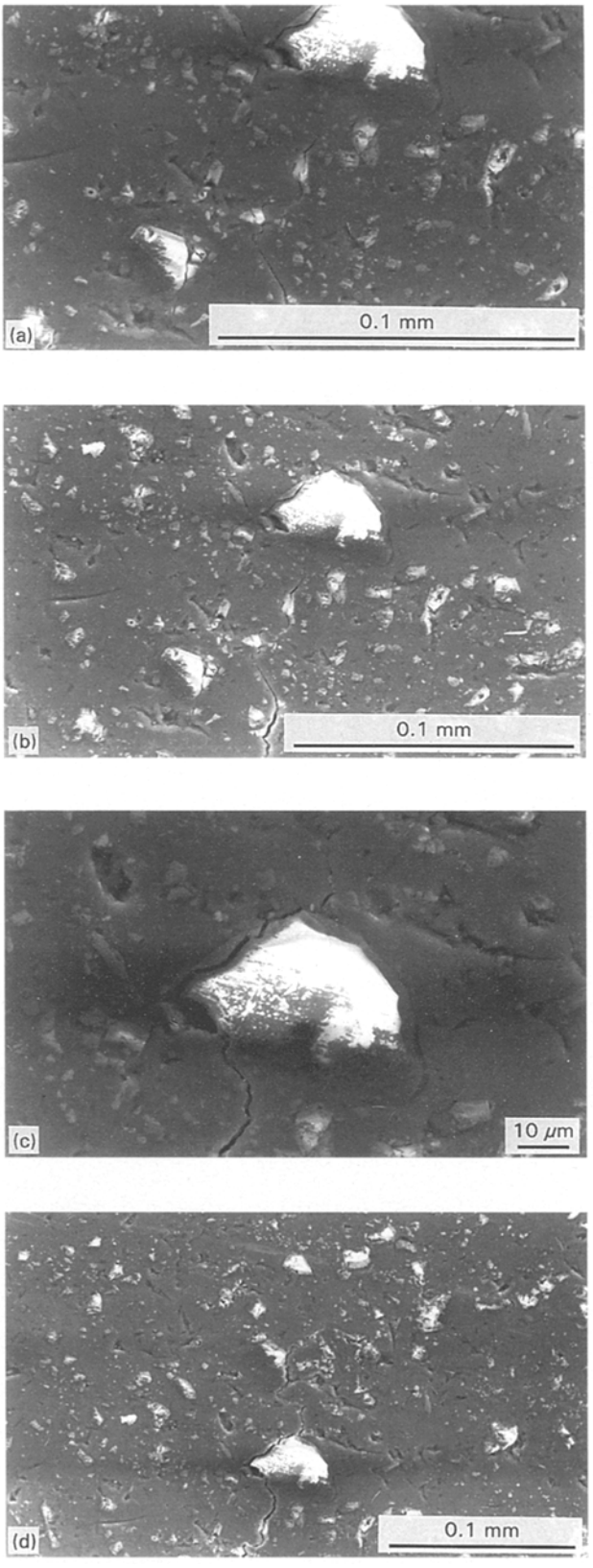

Figure 9 The sequence of crack growth in as-received D20 at low ΔK levels. (a) A crack approaches an alumina particle in front of the crack ($\Delta K = 7.6$ MPa m$^{1/2}$); (b) the crack grows near to the particle; (c) the crack is deflected and links up with another crack in the m/p interface of the particle; (d) the crack continues to grow, passing through the m/p interface of the next particle.

m/p interfaces. At this level of ΔK, crack tip branching was observed. At high levels of ΔK, fatigue cracks grew, due to subcracking ahead of the main crack, which later linked up with the main crack (Fig. 15).

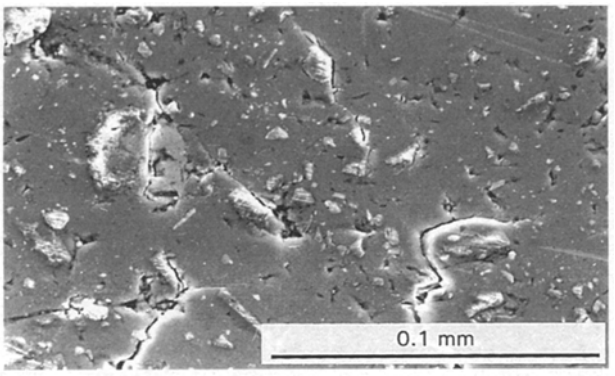

Figure 10 Subcracks ahead of the main crack tip in as-received D20 at high levels of ΔK ($\Delta K = 11.2$ MPa m$^{1/2}$).

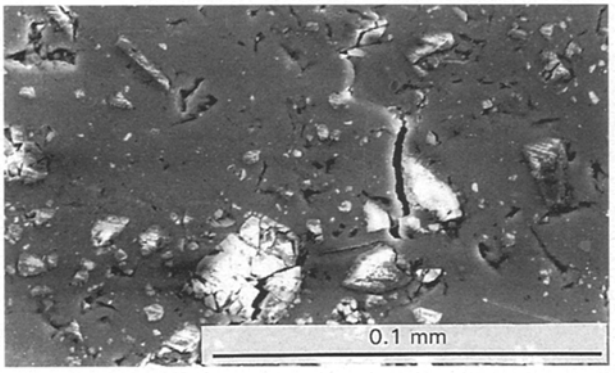

Figure 11 Crack deflection due to the reinforcement phase (as-received condition).

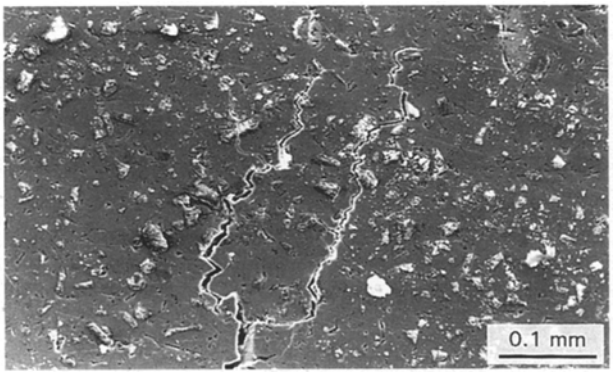

Figure 12 Multiple crack tips in as-received D20 at high levels of ΔK ($\Delta K = 12.4$ MPa m$^{1/2}$).

TABLE I Particle density in the cracked areas

Material	Condition	ΔK levels	Average particle density (10^{-4} μm^{-2})
D20	As-received	Low	6.12
		High	6.98
	T6	Low	6.34
		High	6.99
	Thermal exposed	Low	5.71
		High	6.85
C85	As-received	Low	6.30
		High	6.93
	T6	Low	6.5
		High	7.15
	Thermal exposed	Low	5.8
		High	7.1

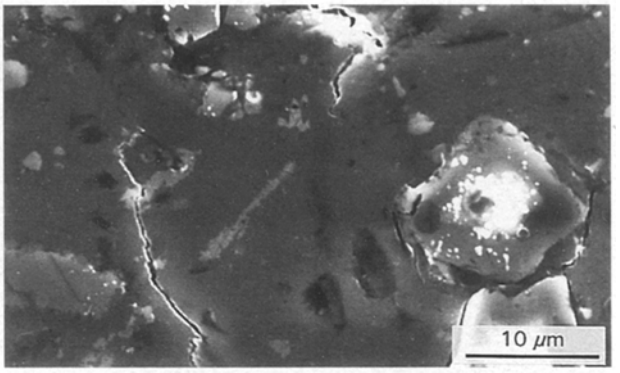

Figure 13 Interface cracking ahead of the crack tip in D20 (T6 condition).

TABLE II Percentage of fractured and debonded reinforcement particles along the fatigue crack path

Material	Condition	Fractured particles (%)	Debonded particles
D20	As-received	12	88
D20	T6	7.3	92.7
D20	Thermally exposed	4.8	95.2
C85	As-received	9.7	90.3
C85	T6	5.6	94.4
C85	Thermally exposed	3.3	96.7

Crack tip branching and microcracking around the main crack was also pronounced at high levels of ΔK. Multiple crack tips, which were found in as-received and T6 specimens, were not observed in thermally exposed specimen at high levels of ΔK. Image analysis results (Table II) indicate that the number of debonded particles in this specimen is higher than in both the as-received and T6 conditions.

3.3. Comral-85 (C85) composite

In the as-received condition, the crack usually passed through m/p interfaces. While at low levels of ΔK the crack went past areas with a slightly lower density of particles, it passed through relatively high particle density areas at high levels of ΔK (Table I). At low levels of ΔK, only a single crack tip was observed. In addition, microcracks near and around the main crack and crack tip branching were found (Fig. 16). Fig. 17 shows a sequence of photographs taken at low levels of ΔK from the as-received specimen showing the effects of particulate reinforcement on crack deflection. In Fig. 17a the crack grew away from the m/p interface of one alumina particle in the matrix; and after 5679 cycles it came near another alumina particle and appeared to cut the particle (Fig. 17b). However, after a further 27191 cycles, it reached the m/p interface of this particle but stopped there (Fig. 17c). Then a microcrack appeared at the m/p interface of the next particle ahead of the main crack (Fig. 17d). Finally, the main crack changed its direction and linked up with this microcrack. In the as-received specimen, at high

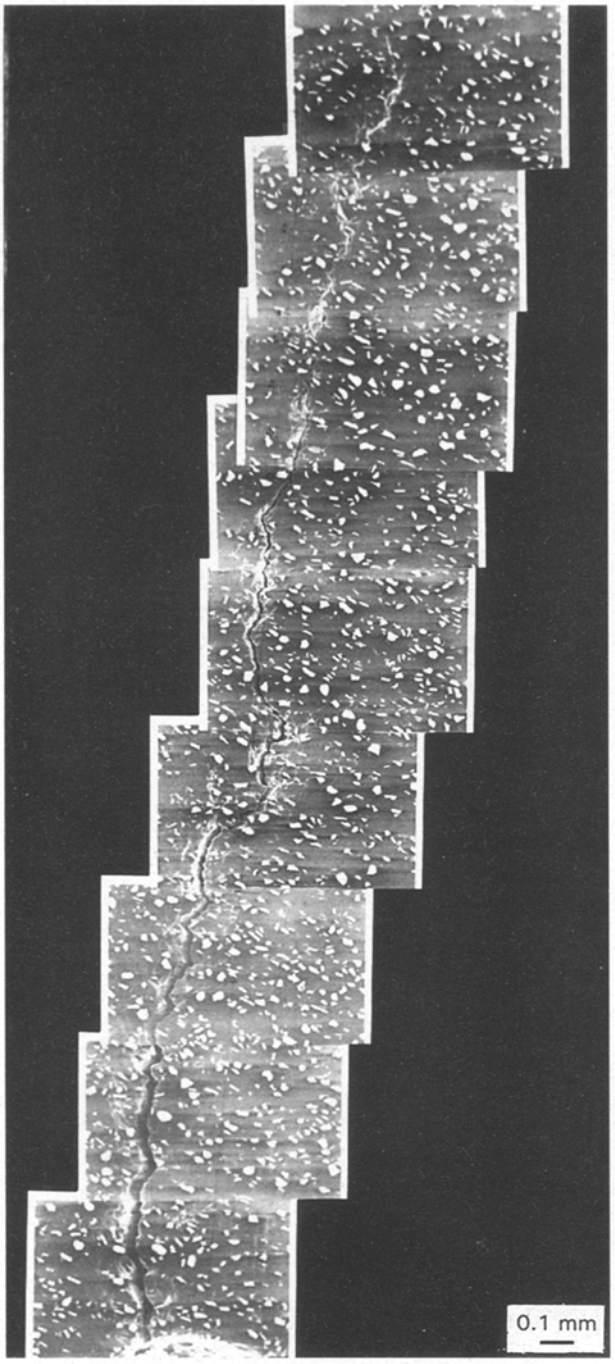

Figure 14 Fatigue crack profile in a thermally exposed D20 specimen.

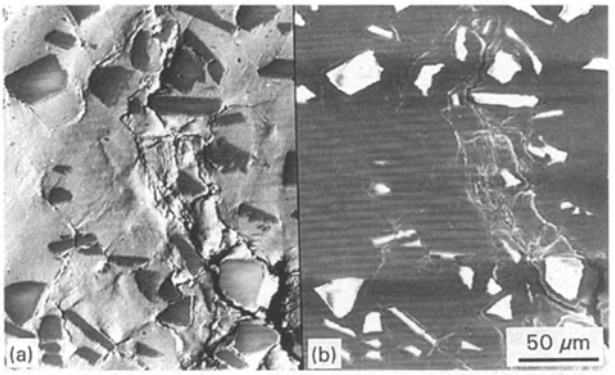

Figure 15 (a) Back scattered and (b) secondary electron image from subcracking ahead of the main crack at high levels of ΔK in thermally exposed D20.

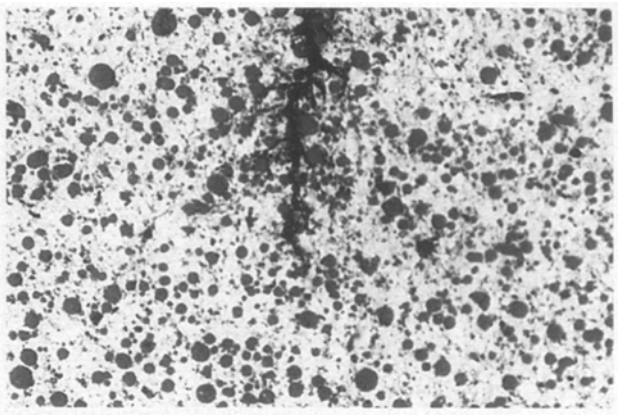

Figure 16 Crack tip branching at low levels of ΔK in as-received C85 ($\Delta K = 6.3$ MPa m$^{1/2}$).

levels of ΔK, again the crack grew mainly due to subcracking ahead of the main crack which coalesced with the main crack. These subcracks were usually initiated at fractured and/or debonded large particles ahead of the crack tip. In addition, at this level of ΔK, more crack tip branching was observed than at low levels of ΔK. Furthermore, multiple crack tips (Fig. 18) were also found at high levels of ΔK.

In the T6 condition, the crack growth behaviour was the same as the as-received material at both high and low levels of ΔK. Image analysis results demonstrate that more particles were debonded from the m/p interface in the T6 condition than in the as-received condition (94.4% compared to 90.3%). Debonded particles in this specimen are shown in Fig. 19. Fig. 20 shows crack deflection at low levels of ΔK in T6 specimen. Fewer crack branches and less microcracking around the main crack were observed in the T6 specimen compared to the as-received specimen.

In the thermally exposed specimen, crack growth was strongly associated with debonded particles from the m/p interface at both low and high levels of ΔK. While at low levels of ΔK the crack grew with a single tip and passed through low particle density areas, at high levels of ΔK, crack growth was sometimes associated with multiple crack tips, high level of crack branching and microcracking ahead and around the main crack. Figs 21 and 22 show microcracks around the crack tip and debonded particles in the crack path, respectively, at high levels of ΔK. In contrast with as-received and T6 condition samples, more crack branching, microcracking and particle debonding were observed in thermally exposed specimen with fewer fractured particles and multiple crack tips. Table II shows the results of image analysis on the crack path of these specimens.

3.4. Fatigue crack growth analysis

The fatigue crack growth rates (da/dN) were calculated by the secant method according to ASTM Standard E647 and plotted (in mm cycle^{-1}) against the maximum stress amplitude ($\Delta K = K_{max}$ and in MPa m$^{1/2}$) for all the tested materials. The results are shown in Fig. 23 for the as-received materials, Fig. 24

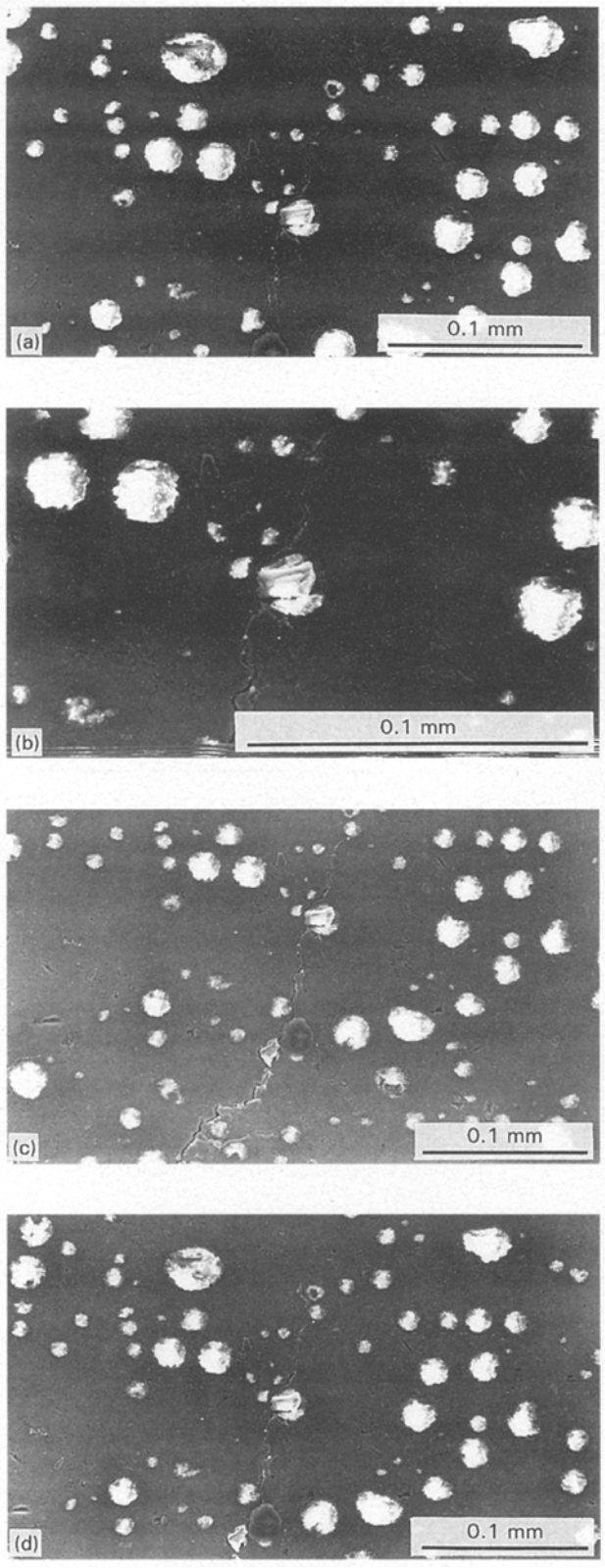

Figure 17 The sequence of fatigue crack growth in as-received C85. (a) The crack grew in the matrix away from alumina particles ($\Delta K = 5.9\ \mathrm{MPa\,m^{1/2}}$); (b) the crack tip approached one alumina particle and appeared to cut the particle; (c) the crack stopped at the m/p interface of the particle; (d) a microcrack appeared at the m/p interface of the next particle ahead of the main crack.

for T6 materials and Fig. 25 for thermally exposed materials. The threshold stress intensity factors, (ΔK_{th}), were estimated from the data at low crack growth rates. The general behaviour of both reinforced and unreinforced materials in all conditions

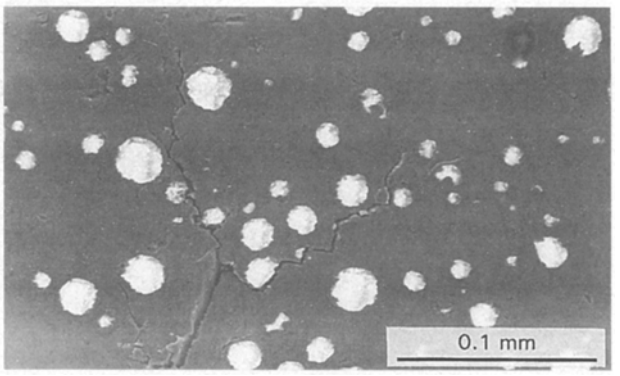

Figure 18 Multiple crack tips at high levels of ΔK in as-received C85 ($\Delta K = 10.2\ \mathrm{MPa\,m^{1/2}}$).

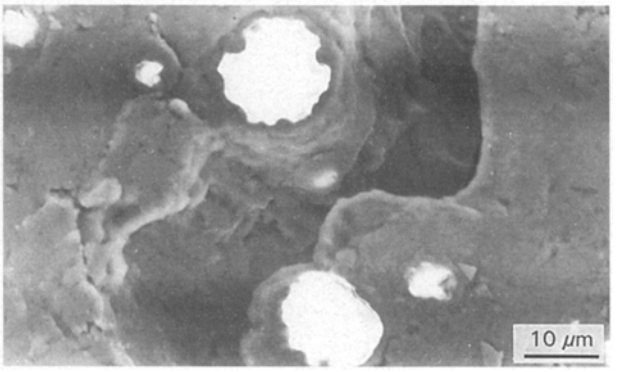

Figure 19 Crack deflection due to m/p interface debonding in C85 T6 condition.

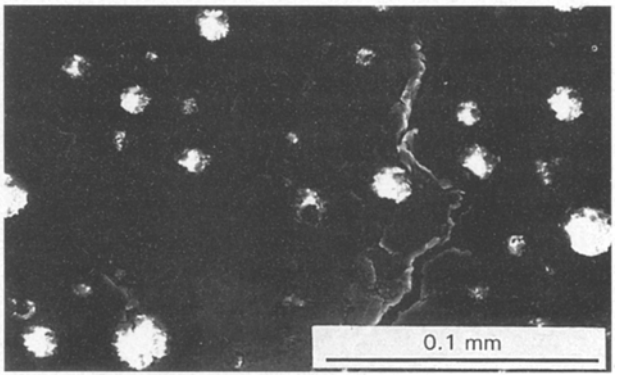

Figure 20 Crack deflection at low levels of ΔK in C85 T6 condition ($\Delta K = 6.1\ \mathrm{MPa\,m^{1/2}}$).

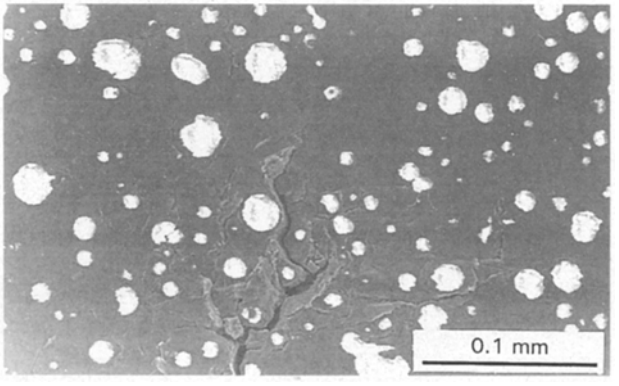

Figure 21 Back-scattered electron image from the crack tip at high levels of ΔK in C85 thermally exposed ($\Delta K = 11.8\ \mathrm{MPa\,m^{1/2}}$).

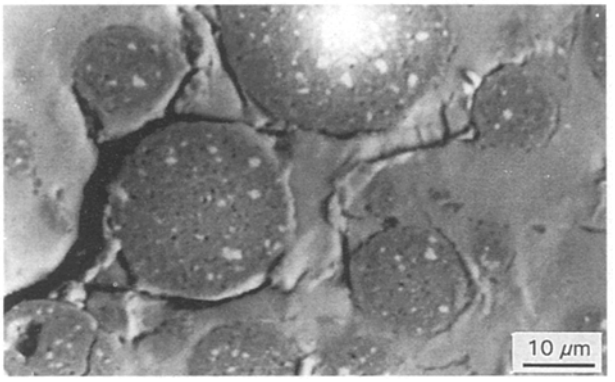

Figure 22 Secondary electron image from debonded particles in thermally exposed C85.

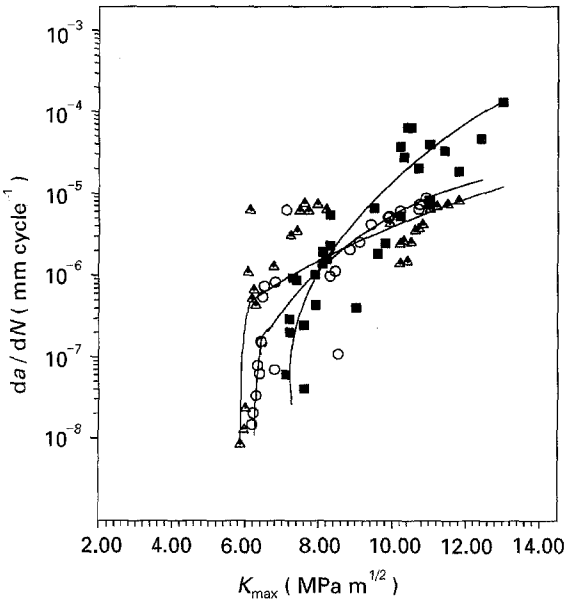

Figure 23 Fatigue crack growth rates (da/dN) versus applied stress intensity range ($\Delta K = K_{max}$) for as-received materials: Δ 6061 Al, (○) Comral-85, (■) Duralcan–20%.

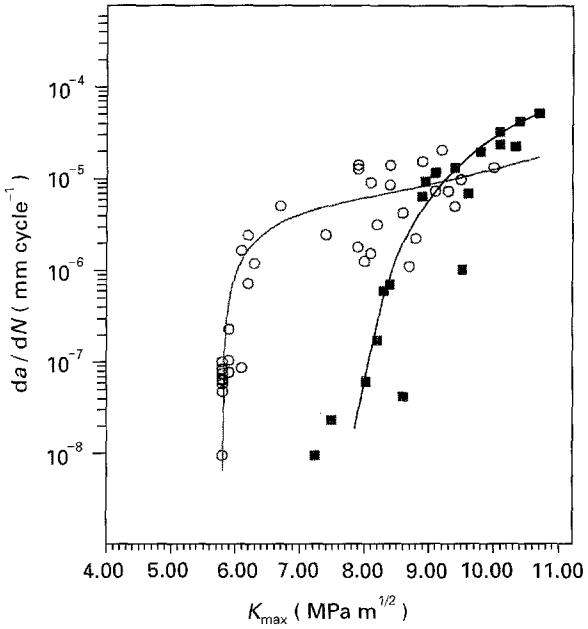

Figure 24 Fatigue crack-growth rates (da/dN) versus applied stress intensity range ($\Delta K = K_{max}$) for MMCs in the T6 condition: (■) Duralcan–20%, (○) Comral-85.

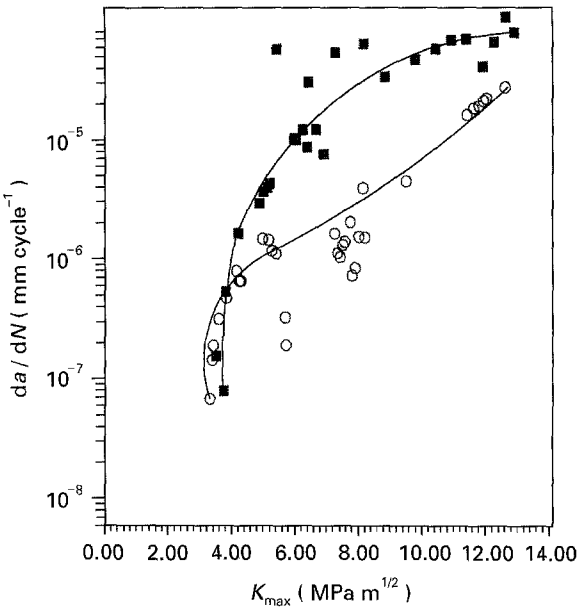

Figure 25 Fatigue crack growth rates (da/dN) versus applied stress intensity range ($\Delta K = K_{max}$) for thermally exposed MMCs at 300 °C for 110 h: (○) Comral-85, (■) Duralcan–20%.

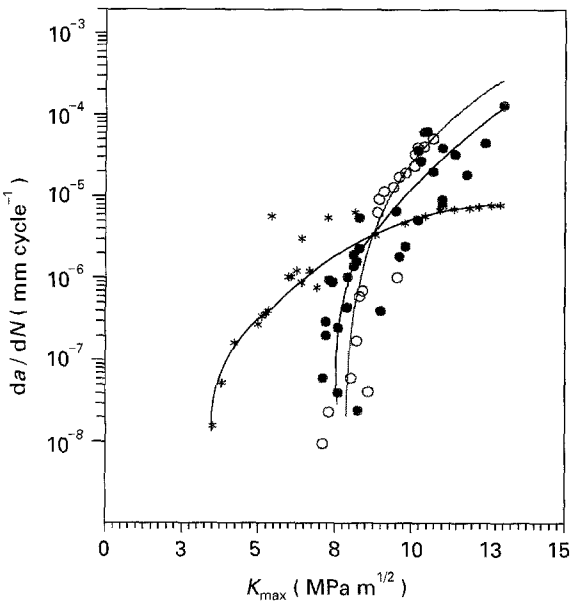

Figure 26 Fatigue crack growth rates (da/dN) versus applied stress intensity range ($\Delta K = K_{max}$) for D20 in three different conditions: (*) thermally exposed, (●) as-received, (○) T6.

examined was typical of metals. In the as-received condition, MMCs exhibit greater ΔK_{th} values and better fatigue crack resistance in the near-threshold region than the unreinforced material. On the other hand, the composites were found to exhibit faster crack growth rates in the Paris region than the unreinforced matrix. This means that the incorporation of ceramic reinforcement in the metal matrix has resulted in higher values of the threshold stress intensity range, below which fatigue cracks are non-propagating, and faster crack growth rates at high levels of ΔK. At the same time, C85 composites show smaller ΔK_{th} values but superior fatigue resistance at high ΔK levels than the D20 composites in all three conditions.

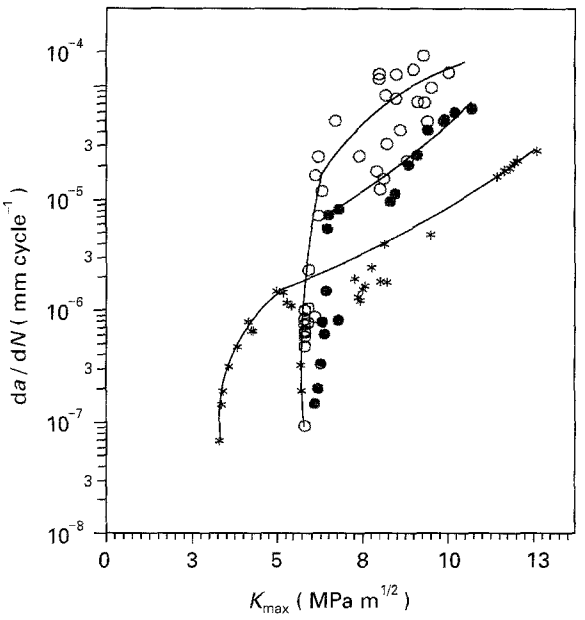

Figure 27 Fatigue crack growth rates (da/dN) versus applied stress intensity range ($\Delta K = K_{max}$) for C85 in three different conditions: (*) thermally exposed, (●) as-received, (○) T6.

Heat treatment to peak-aged condition had very little effect on the threshold value and near-threshold fatigue crack growth, but it accelerated fatigue crack growth in the Paris region for both composite materials (see Figs 26 and 27).

Long-term thermal exposure had a strong effect on the fatigue threshold, near-threshold fatigue crack growth and crack growth rates in the Paris region, for both MMCs. While thermal exposure decreased ΔK_{th}, it reduced fatigue crack growth rates in the Paris region. Figs 26 and 27 show the fatigue crack growth rates of the two MMCs heat treated at different conditions as a function of the applied stress intensity factor range ($\Delta K = K_{max}$).

4. Discussion

The experimental results indicate that the fatigue crack growth rate curves for the tested composites are generally similar in shape to the monolithic alloys. The data scatter is larger than expected and can be attributed to the local microstructure, non-uniform distribution of particles and different particle size and spacing. In conventional fatigue testing, the crack grows long enough to smooth out any local variations with a consequent reduction in scatter. The main purpose of this work was to investigate the micromechanisms of fatigue crack growth in ceramic particulate-reinforced metal-matrix composites. The contribution of the ceramic reinforcement to crack initiation and the mode of crack growth that occurs in a given composite material depends upon the properties of the matrix, the reinforcement phase and the metal/particle interfaces. In addition, the mode and amplitude of the applied stress intensity range is an important factor in determining the crack growth mechanism. The effects of some important factors on fatigue behaviour of the tested materials are discussed in the following sections.

4.1. Effect of particulate reinforcement

Experimental results suggested that introducing particulate reinforcement to the matrix alloy has two different effects on the fatigue behaviour. It increases the threshold stress intensity factor, decreases crack growth rates in the threshold region but increases crack growth rates in the Paris region.

Fatigue crack growth in composites may occur in the matrix, reinforcement or at the m/p interface. Based on experimental observations, the possibility of crack growth in the reinforcement is negligible. Hence the bonding strength of the m/p interface is an important parameter. If it is greater than the matrix strength the crack grows mainly in the matrix and avoids particles. Otherwise, interface failure occurs as the crack approaches the reinforcement particles. It seems that the initial stage of fatigue damage in the MMC is the debonding of the reinforcement from the matrix. Particles ahead of the crack tip act as stress concentrators and increase the local stress more than the strength of the m/p interface. At low ΔK the size of the fracture process zone around the crack tip is small and it envelops only a few particles which are very near to the crack tip. Microcracks are nucleated near and around these particles, therefore particles cannot play an important role to increase the crack growth rates at this stage. At high stress intensity ranges, the size of the fracture process zone is increased, thus more particles can act as stress raisers. Therefore, more microcracks form ahead of the main crack tip at this stage. The results observed here suggest that the interfacial separation together with the fractured particles ahead of the crack tip can be a main factor for microcrack and subcrack initiation which reduce the fatigue resistance of the composite at high levels of ΔK. Williams and Fine [13] also observed that the matrix/whisker interface was a preferential site for crack initiation in a 2124 Al/SiC composite.

Another factor that could also affect crack growth rate, especially at low ΔK values, is crack interaction with reinforcing particles. Cracks are impeded and deflected by reinforcement particles. Crack deflection is one of the mechanisms for toughening of the composite. When the crack tip is deflected from its nominal mode I growth direction, the effective driving force for crack growth is really smaller than that of a straight crack. Therefore, the propagation rate of the deflected crack is reduced. The effect of these interactions becomes less marked with increasing crack length and applied ΔK.

Roughness-induced crack closure has played a significant role in the fatigue process. Figs 28 and 29 show crack closure in D20 and C85 composites in the T6 condition. The higher threshold values and fatigue crack growth behaviour of composites near the threshold region can be explained by this phenomenon. Crack closure is a phenomenon whose influence on fatigue crack growth is strongly dictated by microstructural factors. At low ΔK, when crack tip opening displacements are small compared to the average height of the fracture surface asperities, roughness-induced crack closure is promoted. Permanent plastic deformations ahead of the crack tip, as well as crack

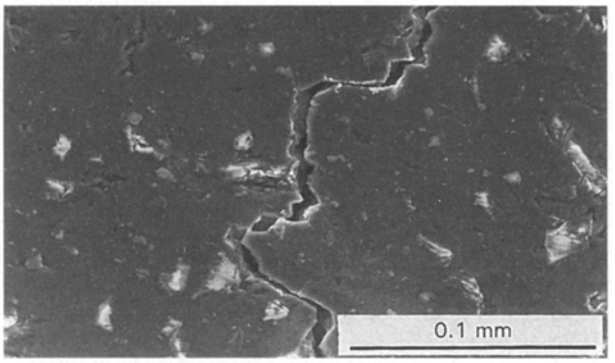

Figure 28 Crack closure in D20 composite, T6 condition.

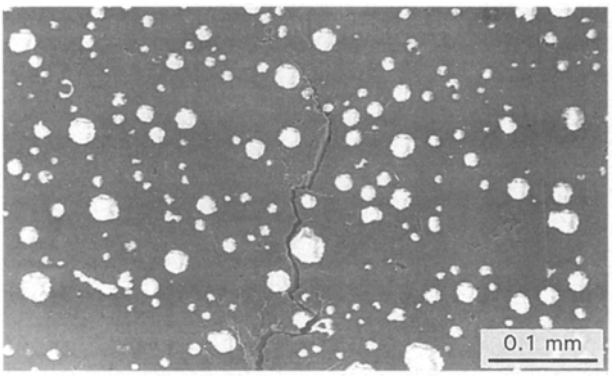

Figure 29 Crack closure in C85 composite, T6 condition.

deflection and debonded particles, cause a mismatch between the fracture surface asperities. It provides a mechanism for enhanced crack closure. At low ΔK levels, even small fluctuations in the microstructural path of the crack by reinforcement particles can cause large fluctuations in crack propagation rates. The most important effects of roughness-induced crack closure occur whenever microstructurally induced crack deflection generates contact between the fracture surfaces (Figs 28 and 29).

The higher fatigue crack growth rates at high levels of ΔK in the composites could be partly explained by the lower fracture toughness of the MMCs [14], which reduces the final stress intensity factor for fast fracture. In addition, the existence of weakly bonded alumina particles, fracture of large particles, crack tip jumping and linking with subcracks, and also rapid propagation of the crack along the particle clusters at high levels of ΔK, can provide further reasons for the inferior fatigue crack resistance of composites at this level of ΔK. Levin and Karlsson [15] also reported a decreased resistance to fatigue crack growth in the composites compared to the unreinforced matrix.

4.2. Effect of ΔK level

The general observation in the present work is that at low stress levels the fatigue crack tends to avoid the alumina particles, passes through relatively low-density particle areas and interacts with the m/p interface. As the stress level is increased the number of particles interacting with the crack increases. Particles ahead of the crack tip fracture and/or debond from the m/p interface and subcracks ahead of the crack tip are produced. The crack growth rate is irregular and crack jumping occurs easily along the areas with a relatively dense population of particles. Cracks grow rapidly due to the coalescence of the main crack with the subcracks. At this stage it is possible to consider the crack tip as located at the further end of the microcracks and treat the ligamentary material between the main crack and microcracks as a bridge. Kumaie *et al.* [10] reported that in 6061 Al/15 vol % SiC at low stress intensity levels, the fatigue cracks tended to run through the matrix and avoided SiC particles, whilst at high stress intensity levels, cracking of SiC particles was observed ahead of the crack tip.

An increasing number of fractured and debonded particles with rising ΔK reflects the increased interaction between the crack tip fracture process zone and the alumina particles. If the fracture process zone is defined as the volume of material ahead of the crack tip in which the stress is sufficient to damage particles (fracture or/and debond from the m/p interface), the size of the fracture process zone increases with ΔK. It is known that the size of the fracture process zone increases in proportion to K^2_{max} [15]. Therefore, the number of particles encountered by the process zone increases remarkably as ΔK rises. In this region only alumina particles directly in contact with the crack tip were found to fracture while the others were separated from the m/p interface, nucleated subcracks, and provided an easy path for crack growth.

4.3. Effect of material condition

Heat treatment from as-received to peak-aged condition was found to have little effect on ΔK_{th} and crack growth rate near the threshold region, but it increased crack growth in the Paris region. Earlier studies by the authors on ageing behaviour, mechanical properties and fracture properties of these MMCs [14, 16, 17] show two different effects of heat treatment. Firstly, heat treatment to peak-aged condition changes the mechanical properties of the matrix, increasing the strength but decreasing the ductility of the MMC material. Secondly, it weakens the m/p interface. Near ΔK_{th} fatigue cracks are associated with the alumina particles debonded at the m/p interface, because the ageing condition does not improve the already poor m/p interface, so it has little influence on the near-threshold fatigue behaviour. On the other hand, ΔK_{th} is largely dependent upon crack closure and crack deflection. Because the D20 and C85 MMCs have similar crack closure behaviour at the as-received and T6 condition, ΔK_{th} is expected to be similar. Vasudevan and Sadananda [18] also observed, in Al–Zn–Mg–Cu/SiC MMC, that ΔK_{th} was insensitive to matrix ageing treatment.

At high levels of ΔK, the lower fracture toughness of the T6 materials, together with a weaker m/p interface in this condition compared to the as-received materials, provide more favourable conditions and easier paths for crack growth in the T6 materials, leading to higher crack growth rates.

Experimental results indicate that thermal exposure at 300 °C for 110 h after peak-aged heat treatment has a strong effect on the fatigue behaviour of the MMCs, decreasing both ΔK_{th} and crack growth rates in the Paris region. Image analysis shows that thermal exposure influences m/p interfaces and makes it even weaker than the T6 condition. At low ΔK levels, the crack avoided particles and mostly passed through the matrix (Table I). This behaviour reduces crack deflection and surface roughness required for crack closure, leading to a low ΔK_{th}. Previous work on the unreinforced matrix alloy [16] indicates that heat treatment in the over-aged condition increases the ductility but reduces the yield strength. Therefore, at high levels of ΔK, higher ductility and lower yield strength of the very much over-aged matrix of the thermally exposed specimens could be the main factor for the lower crack growth rates in these specimens.

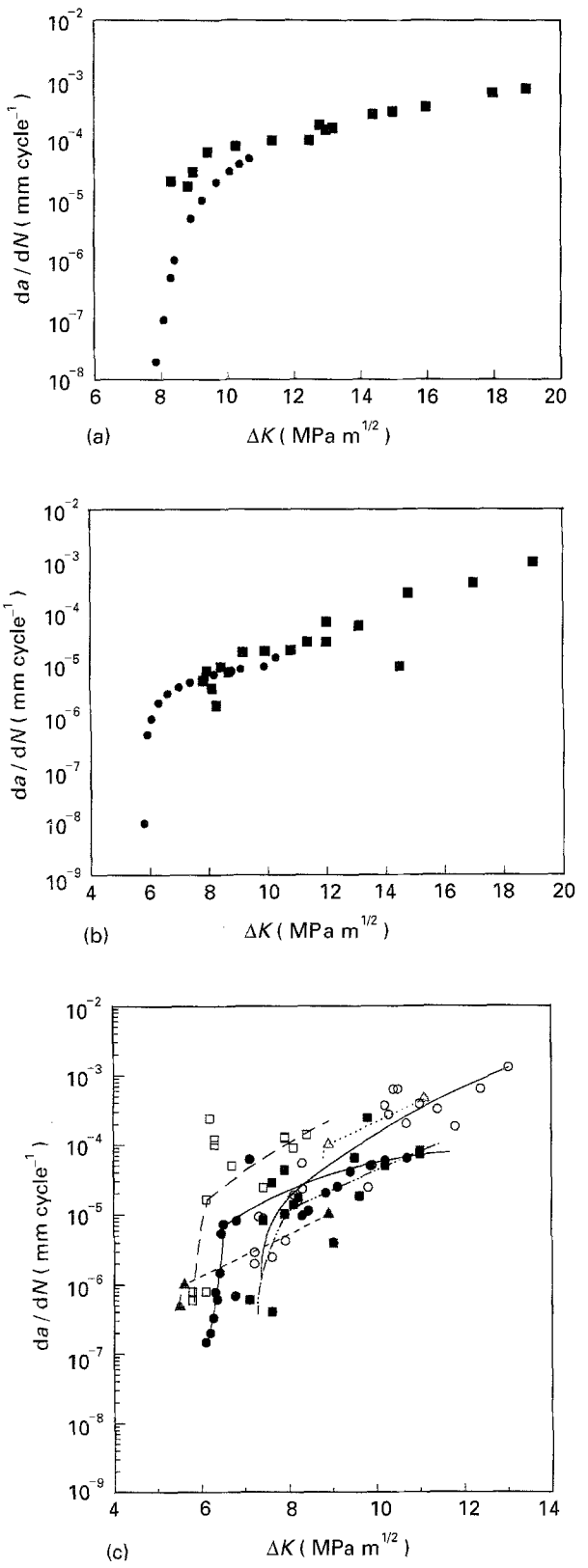

Figure 30 (a, b) Comparison of crack growth rates of this work (in situ SEM technique) with four-point method bend specimens of (a) D20 and (b) C85 in the T6 condition. (c) Comparison of crack growth rates of this work with other published results (○) D20, 20 vol % alumina; (●) C85, 20 vol % alumina; (□) Biner [8], 25 vol % SiC; (■) Duralcan [19], 15 vol % SiC; (△) Logsdon [2], 25 vol % SiC; (▲) Kumai [10], 15 vol % SiC.

4.4. Comparison with other data

Fig. 30a–c show a comparison between results of this work in the T6 condition and other results for 6061 Al matrix reinforced with ceramic particles obtained from the literature. Fig. 30a and b compare the da/dN versus ΔK results for the same Duralcan 20 and Comral 85 materials using the *in situ* SEM technique of this work and the four-point notched bend specimens. The two sets of data overlap each other indicating the reliability of the data obtained by the *in situ* SEM method. Fig. 30c compares the present data with other available results. The data for Duralcan 15 vol % SiC [19] show slightly better crack growth resistance than D20 and C85 and similar ΔK_{th} to D20. The results for 6061 Al/15 vol % SiC [10] lie below the results of D20 and C85 and indicating a higher resistance to fatigue crack growth when compared to the D20 and C85. The results of 6061 Al/25 vol % SiC [2, 8] are both slightly above the results of D20 and C85 and show lower resistance to crack growth. It is interesting to note that resistance to fatigue crack growth, in the relatively high growth rate regimes, is more dependent on the volume fraction of reinforcement phase than on the particulate type. An increase of the volume fraction of reinforcement would decrease the resistance to fatigue crack growth.

5. Conclusions

1. It was observed that both D20 and C85 MMCs in the as-received condition have superior fatigue resistance in the near-threshold region and greater threshold stress intensity values than the unreinforced alloy. However, both MMCs have inferior fatigue resistance in the Paris region when compared to the unreinforced alloy.

2. It seems that in all tested materials, the applied ΔK level has a strong influence on the fatigue crack behaviour. At low levels of ΔK the crack grows with a single crack tip and in areas with a relatively low density of particles. However, at high levels of ΔK, subcracks are seen ahead of the crack tip and they link up with the main crack.

3. The dominant mechanism for crack growth in the MMCs in all tested conditions is particle/matrix interface debonding.

4. Heat treatment of the composites to the peak-aged condition has very little effect on the fatigue threshold values and near-threshold fatigue crack growth. However, long-term thermal exposure at 300 °C decreases the fatigue threshold values and fatigue crack growth rates near the threshold in both D20 and C85 composites. Also, peak-ageing increases but long-term thermal exposure decreases fatigue crack growth rates in the Paris region.

Acknowledgements

The authors thank the Australian Research Council (ARC) for the continuing support of this work, Dr J. Healy for helping with the initial experiments, and Mr G. Heness for kindly providing his notched bend data for comparison in Fig. 30a.

References

1. S. S. YAU and G. MAYER, *Mater. Sci. Eng.* **82** (1986) 45.
2. W. A. LOGSDON and P. K. LIAW, *Eng. Fract. Mech.* **24** (1986) 737.
3. S. V. NAIR, J. K. TIEN and R. C. BATES, *Int. Met. Rev.* **30** (1985) 275.
4. J. K. SHANG and R. O. RITCHIE, *Metall. Trans. A* **20** (1989) 897.
5. D. L. DAVIDSON, *ibid.* **22** (1991) 97.
6. *Idem, Acta Metall.* **36** (1988) 2275.
7. T. CHRISTMAN and S. SURESH, *Mater. Sci. Eng. A* **102** (1988) 211.
8. S. B. BINER, *Fat. Fract. Eng. Mater. Struct.* **13** (1990) 637.
9. J. C. HEALY and C. J. BEEVERS, *Mater. Sci. Eng.* **A142** (1991) 183.
10. S. KUMAI, J. E. KING and J. F. KNOTT, *Fat. Fract. Eng. Mater. Struct.* **13** (1990) 511.
11. O. Ø. MOURITSEN and B. L. KARIHALOO, *Mater. Forum* **15** (1990) 360.
12. Y. MURAKAMI, "Stress Intensity Factors Handbook" (Pergamon Press, Oxford, 1986).
13. D. R. WILLIAMS and M.E. FINE, in "Proceedings of the 5th International Conference on Composite Materials", edited by W. C. HARRIGAN, J. STRLEF and A. K. DHINGRA (1985) p. 639.
14. M. J. HADIANFARD, G. HENESS, J. HEALY and Y. M. MAI, *Fat. Fract. Eng. Mater. Struct.* **17** (1994) 253.
15. M. LEVIN and B. KARLSSON, *Mater. Sci. Technol.* **7** (1991) 596.
16. M. J. HADIANFARD, PhD thesis, Sydney University, Australia (1995).
17. M. J. HADIANFARD, J. HEALY and Y. W. MAI, in "Proceedings of Advanced Composite 93", Wollongong, Australia, edited by T. CHANDRA, A.K. DHINGRA (TMS, Warrendale, PA, 1993) pp. 1199–206.
18. A. K. VASUDEVAN and K. SADANANDA, *Scripta Metall. Mater.* **28** (1993) 837.
19. Duralcan data sheet, Duralcan USA, 10505 Roselle Street, San Diego, CA 92121 (1990).

Received 12 April
and accepted 2 May 1995